Cellular Morphogenesis Under Stress Is Influenced by the Sphingolipid Pathway Gene *ISC1* and DNA Integrity Checkpoint Genes in *Saccharomyces cerevisiae*

Kaushlendra Tripathi, Nabil Matmati, W. Jim Zheng, Yusuf A. Hannun, and Bidyut K. Mohanty[1]
Department of Biochemistry and Molecular Biology, Medical University of South Carolina, Charleston, South Carolina 29425

ABSTRACT In *Saccharomyces cerevisiae*, replication stress induced by hydroxyurea (HU) and methyl methanesulfonate (MMS) activates DNA integrity checkpoints; in checkpoint-defective yeast strains, HU treatment also induces morphological aberrations. We find that the sphingolipid pathway gene *ISC1*, the product of which catalyzes the generation of bioactive ceramides from complex sphingolipids, plays a novel role in determining cellular morphology following HU/MMS treatment. HU-treated *isc1*Δ cells display morphological aberrations, cell-wall defects, and defects in actin depolymerization. Swe1, a morphogenesis checkpoint regulator, and the cell cycle regulator Cdk1 play key roles in these morphological defects of *isc1*Δ cells. A genetic approach reveals that *ISC1* interacts with other checkpoint proteins to control cell morphology. That is, yeast carrying deletions of both *ISC1* and a replication checkpoint mediator gene including *MRC1*, *TOF1*, or *CSM3* display basal morphological defects, which increase following HU treatment. Interestingly, strains with deletions of both *ISC1* and the DNA damage checkpoint mediator gene *RAD9* display reduced morphological aberrations irrespective of HU treatment, suggesting a role for *RAD9* in determining the morphology of *isc1*Δ cells. Mechanistically, the checkpoint regulator Rad53 partially influences *isc1*Δ cell morphology in a dosage-dependent manner.

THE baker's yeast *Saccharomyces cerevisiae* is dimorphic, existing in budding or pseudohyphal form, depending on its environment. In response to environmental cues such as nitrogen starvation or the presence of short-chain alcohols, diploid and certain haploid strains of yeast undergo morphological differentiation from budding to pseudohyphal forms (Gimeno *et al.* 1992; Lorenz *et al.* 2000; Lew 2003; Bharucha *et al.* 2008). MAPK and cAMP pathways are important in inducing such pseudohyphal growth in response to these environmental cues (Liu *et al.* 1993; Roberts and Fink 1994; Ward *et al.* 1995; Lengeler *et al.* 2000; Lorenz *et al.* 2000; Pan *et al.* 2000; Pan and Heitman 2002; Bharucha *et al.* 2008).

A morphogenesis checkpoint allows the cell to monitor defects in bud morphology, actin cytoskeleton perturbations, and cell-wall synthesis (Lew and Reed 1995) through its key regulator, Swe1 protein kinase (Lee *et al.* 2005; Keaton *et al.* 2007). Swe1 phosphorylates and inactivates Cdk1 at Tyr19 to cause cell cycle delay and to control morphogenetic irregularities. Swe1 accumulation is initiated in early S phase and its degradation must occur at the end of the G2 phase for the G2/M transition to occur (Sia *et al.* 1998; Lee *et al.* 2005). Persistence of Swe1 causes prolonged inhibition of Cdk1, which, in turn, can induce pseudohyphal growth (Pruyne and Bretscher 2000a,b).

Exposure to hydroxyurea (HU) or methyl methanesulfonate (MMS), both of which slow DNA synthesis, has been shown to induce minor morphological aberrations in yeast, specifically semifilamentous growth in certain wild-type strains (Jiang and Kang 2003), although most haploid wild-type strains tested undergo no morphological changes after HU exposure (Enserink *et al.* 2006). Both HU and MMS impede progression of DNA replication machinery, slow S-phase progression, and can induce DNA damage (Tercero and Diffley 2001; Katou *et al.* 2003; Zegerman and Diffley 2003). Cells respond to these genotoxic agents by activating checkpoints that cause cell cycle arrest while activating DNA

doi: 10.1534/genetics.111.132092
Manuscript received June 27, 2011; accepted for publication August 5, 2011
Supporting information is available online at http://www.genetics.org/content/suppl/2011/08/12/genetics.111.132092.DC1.
[1]Corresponding author: Department of Biochemistry and Molecular Biology, Medical University of South Carolina, 173 Ashley Ave., Charleston, SC 29425.
E-mail: mohanty@musc.edu

Table 1 Strains and plasmids

Strains	Genotype	Reference
Jk9-3d a	*MAT***a** *trp1 leu2-3 his4 ura3 ade2 rme1*	Matmati *et al.* (2009)
JK9-3d a *isc1*Δ	JK9-3d a *isc1*::KanMX	Matmati *et al.* (2009)
JK9-3d a *tof1*Δ	JK9-3d a *tof1*:: KanMX	This study
JK9-3d a *mrc1*Δ	JK9-3d a *mrc1*::KanMX	This study
JK9-3d a *csm3*Δ	JK9-3d a *csm3*::KanMX	This study
JK9-3d a *rad9*Δ	JK9-3d a *rad9*::KanMX	This study
JK9-3d a *swe1*Δ	JK9-3d a *swe1*::KanMX	This study
JK9-3d a *isc1*Δ*tof1*Δ	JK9-3d a *isc1*:: KanMX *tof1*Δ::Phl	This study
JK9-3d a *isc1*Δ*mrc1*Δ	JK9-3d a *isc1*:: KanMX *mrc1*Δ::Phl	This study
JK9-3d a *isc1*Δ*csm3*Δ	JK9-3d a *isc1*:: KanMX *csm3*Δ::Phl	This study
JK9-3d a *isc1*Δ*swe1*Δ	JK9-3d a *isc1*:: KanMX *swe1*Δ::Phl	This study
JK9-3d a *isc1*Δ*bem1*Δ	JK9-3d a *isc1*:: KanMX *bem1*Δ::Phl	This study
JK9-3d a *isc1*Δ*bni1*Δ	JK9-3d a *isc1*:: KanMX *bni1*Δ::Phl	This study
JK9-3d a *isc1*Δ*rad9*Δ	JK9-3d a *isc1*:: KanMX *rad9*Δ::Phl	This study
JK9-3d α	*MAT*α *trp1 leu2-3 his4 ura3 ade2 rme1*	Sawai *et al.* (2000)
JK9-3d α *isc1*Δ	JK9-3d α *isc1*:: KanMX	Sawai *et al.* (2000)
BY4741	*MAT***a** *his3*Δ*1*; *leu2*Δ*0*; *met15*Δ*0*; *ura3*Δ*0*	Invitrogen
BY4741 *isc1*Δ	BY4741 *isc1*:: KanMX	Invitrogen

Plasmids	Gene	Reference
pRS316-*ISC1*	*ISC1*	Vaena de Avalos *et al.* (2004)
pBG999	*COF1-GFP*	Gandhi *et al.* (2009)
pJM1042 [*CDC28*]	WT *CDK1*	McMillan *et al.* (1999)
pAL88 [*CDC28Y19F*]	*Cdk1Y19F*	McMillan *et al.* (1999)
pRS315	*LEU2*-CEN-*ARS4*	Sikorski and Heiter (1989)
pCla6	*RAD53*-CEN-*LEU2*	Diani *et al.* (2009)

repair machinery (Weinert and Hartwell 1988; Branzei and Foiani 2007). Furthermore, recent studies have shown that checkpoint proteins also play a role in morphogenesis in *S. cerevisiae* and *Candida albicans* (Jiang and Kang 2003; Enserink *et al.* 2006; Smolka *et al.* 2006; Shi *et al.* 2007) in addition to their role in cell cycle arrest and DNA repair (Wang 2009).

Many genes are involved in DNA damage checkpoint activity and morphogenesis, only some of which have been identified. In *S. cerevisiae*, DNA damage is identified by sensor proteins Mec1 and Tel1, which signal through the mediator Rad9 to downstream effectors Rad53 and Chk1 (Putnam *et al.* 2009). Three important components of the DNA replication machinery—Mrc1, Tof1, and Csm3—act as the replication checkpoint mediators in the place of Rad9 (Alcasabas *et al.* 2001; Katou *et al.* 2003; Bando *et al.* 2009). These mediators appear to function differently during normal DNA replication from when they are activated as part of a checkpoint (Katou *et al.* 2003; Calzada *et al.* 2005; Szyjka *et al.* 2005; Tourriere *et al.* 2005; Mohanty *et al.* 2006; Bando *et al.* 2009; Tanaka *et al.* 2009). Genome-wide studies reveal that, in addition to genes controlling cell cycle checkpoints, genes from other pathways such as amino acid, carbohydrate, and lipid metabolism also contribute to HU and MMS resistance (Chang *et al.* 2002; Hanway *et al.* 2002; Parsons *et al.* 2004). Genes in the sphingolipid pathway have been found to confer resistance to HU and MMS (Chang *et al.* 2002; Hanway *et al.* 2002).

Sphingolipids not only have major structural roles in the cell, but also are important bioactive molecules involved in signaling (Futerman and Riezman 2005; Riezman 2006; Milhas *et al.* 2009). Isc1 is the sole inositol phosphosphingolipid-phospholipase C protein identified in yeast that converts complex sphingolipids to ceramides; it is the ortholog of the mammalian neutral sphingomyelinases (Sawai *et al.* 2000; Matmati and Hannun 2008). Deletion of *ISC1* in yeast causes sensitivity to HU and MMS and G2/M arrest (Matmati *et al.* 2009). HU-mediated G2/M block of *isc1*Δ cells can be rescued by deleting the *SWE1* gene or by expressing a non-phosphorylatable Tyr-19 mutant of Cdk1 (Matmati *et al.* 2009).

We report that deletion of the *ISC1* gene leads to morphological aberrations in *S. cerevisiae* cells upon exposure to various agents such as HU, MMS, galactose, or butanol. Morphological defects occurring after treatment with HU, galactose, or butanol are associated with stabilization of the morphogenesis checkpoint regulator Swe1; deletion of the *SWE1* gene abolishes defects under all stress conditions tested. The aberrations induced upon replication stress by HU are associated with modification of the actin cytoskeleton and cell wall. Deletion of the replication checkpoint mediator genes *MRC1*, *TOF1*, or *CSM3* does not reduce morphological defects significantly in *isc1*Δ cells after HU treatment; instead, these cells have morphological irregularities and cell-wall defects under unperturbed conditions. In contrast, deletion of *RAD9* in *isc1*Δ cells reduces morphological

defects significantly with HU treatment, although it does not reduce HU sensitivity. Finally, checkpoint effector Rad53 plays an important role in morphological defects of *isc1Δ* cells under HU stress. Such results indicate the importance of a sphingolipid gene in the control of cellular morphogenesis under various stress conditions.

Materials and Methods

Strains and plasmids

All strains and plasmids are listed in Table 1. Gene deletions were produced using G418 and phleomycin cassettes (Longtine *et al.* 1998; Gueldener *et al.* 2002).

Construction of double-deletion strains in isc1Δ background

Plasmid pRS416-*ISC1* containing the *ISC1* gene, including its endogenous promoter (Vaena De Avalos *et al.* 2004), was transformed into the *isc1Δ* derivative of Jk9-3d a. The *CSM3*, *TOF1*, *MRC1*, or *RAD9* gene was then deleted from this strain using a phleomycin cassette. To subsequently select for loss of pRS416-*ISC1*, cells were grown in SD/Ura$^-$ media followed by growth in YPD media, and cells were plated on SC plates containing 5-FOA.

Microscopy

Live cells grown in rich or minimal media were visualized under a Nikon Eclipse (TE2000-5) microscope with ×400 magnification. For all other purposes, cells were fixed with 3.7% formaldehyde, washed with phosphate buffer (50 mM, pH 7), and suspended in phosphate buffer. Formaldehyde-fixed cells were stained with calcofluor white (CFW; Sigma) at a final concentration of 50 μg/ml and visualized by ×1000 magnification at excitation and emission wavelength of 350 and 550 nm, respectively. For visualization of the actin cytoskeleton, fixed cells were stained with rhodamine–phalloidin (Invitrogen) according to the manufacturer's instructions and visualized by ×1000 magnification at excitation and emission wavelengths of 525–545 and 565 nm, respectively. For visualization of nuclei, cells were stained with DAPI (Vectashield) and examined by ×1000 magnification at excitation and emission wavelengths of 355 and 455/525 nm, respectively.

Analysis of morphological aberrations

Overnight cultures were inoculated into fresh YPD at 1:20 dilution and grown at 30° to an A_{600} of 0.4, when agents were added to the following final concentrations: 12.5–200 mM HU (Sigma), 0.033% v/v MMS (Sigma), 1% v/v 1-butanol, or 2.0% D-galactose (Sigma). For galactose experiments, log-phase cells were pelleted, washed with medium containing yeast extract and peptone (without glucose), and grown in yeast extract–peptone–galactose medium. Cells containing pRS315 or pCla6 were grown overnight in SD/Leu$^-$ medium, inoculated into fresh SD/Leu$^-$ medium, and grown to an A_{600} of 0.2 when HU was added to 12.5 or 25 mM. Cells were collected at 5 and 22 hr after HU/MMS exposure or after 17 hr of butanol and galactose exposure, fixed with 3.7% formaldehyde, and washed with phosphate buffer before visualization. A bud was considered elongated if its length was more than two times its width (Enserink *et al.* 2006). The percentage of elongated buds or cells with abnormal morphology was calculated from large-budded populations only; populations containing only unbudded and small-budded cells were not considered.

Growth rates

Overnight cultures were inoculated in fresh YPD to an A_{600} of 0.2, and absorbance (A_{600}) was measured at 3, 6, 9, and 12 hr growth at 30°. Cells containing pRS315 or pCla6 were grown in SD/Leu$^-$ medium as described above. Experiments were repeated at least five times.

Sensitivity to HU, MMS, and CFW

YPD plates containing 100 or 200 mM HU, 0.033% (v/v) MMS, or 8 mM CFW were prepared and used within 48 hr of preparation. Overnight cultures were inoculated in fresh YPD medium at an A_{600} of 0.2 and grown at 30°. Log-phase cultures were adjusted to an A_{600} of 0.4 before making 10-fold serial dilutions and spotting 2.5 μl each on the plates. Cells containing plasmids such as pCla6 (Diani *et al.* 2009) were grown in SD/Leu$^-$ medium; SD/Leu$^-$ plates contained 25 or 50 mM HU.

Western blot analysis

Cell extracts were prepared from log-phase cultures as described previously (Matmati *et al.* 2009). An equal amount of each protein extract was fractionated by SDS-PAGE, blotted, and probed for Swe1 protein as previously described (Matmati *et al.* 2009). The Pstaire antibody (Santa Cruz) that recognizes amino acid residues 45–51 of Cdc2-p34 was used as a control in all Western blot analyses. Samples were also run through SDS-PAGE in parallel to compare protein concentrations using Coomassie blue staining.

Results

Replication stress induces aberrant morphology in isc1Δ cells

Strains containing *ISC1* gene deletions are sensitive to genotoxic agents HU and MMS in long-term exposure tests (Matmati *et al.* 2009). We observed that *isc1Δ* cells developed many morphological aberrations after exposure to either HU or MMS. Wild-type (WT) cells exposed to HU or MMS display modest elongation of mother cell or buds only after 22 hr of HU exposure. In contrast, *isc1Δ* cells had many morphological abnormalities after exposure to either HU or MMS for 5 or 22 hr (Figure 1, A and B). The morphological changes could even be seen as early as 3 hr after genotoxic treatment (data not shown). Abnormalities included elongated buds, seen in 60% of cells 22 hr post-HU treatment, and daughter cells that did not separate from mother cells,

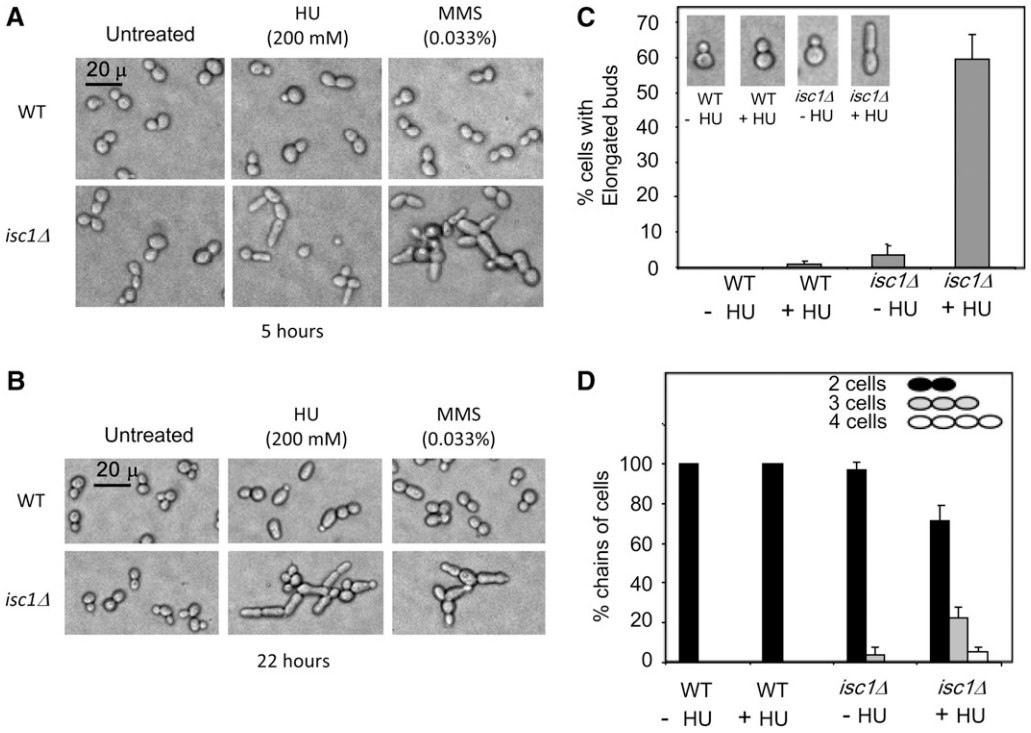

Figure 1 HU and MMS induce morphological aberrations in *isc1*Δ cells. (A) Cellular morphology after a 5-hr exposure of WT and *isc1*Δ cells to HU or MMS (phase contrast ×400). (B) Cellular morphology after a 22-hr exposure to HU and MMS (phase contrast ×400). (C) Bars depict the frequency of elongated bud formation in *isc1*Δ cells exposed to HU for 22 hr. (D) Bars depict the frequency of chains containing three or more cells in *isc1*Δ cells after HU exposure for 22 hr.

resulting in chain-like structures of three or more cells (Figure 1C). After 22 hr of HU treatment, ~22% of the cells were found in three-cell chains and ~5% in four-cell chains (Figure 1D). Often the bud attached to the mother cell was highly elongated. In the absence of HU treatment, a small population of *isc1*Δ cells (~3%) had elongated buds and three-cell chains (Figure 1, C and D; 200–500 cells were counted in each sample for morphological defects). Perhaps these cells have experienced replication stress, DNA damage, or other types of stress and are more sensitive to that stress in the absence of *isc1*.

The pattern of HU-induced morphological abnormalities was also observed in *isc1*Δ cells of the Jk9-3d "α" mating type as well as in *isc1*Δ cells of BY4741; wild-type cells of each strain did not undergo significant morphological change, whereas *isc1*Δ cells formed elongated buds and chains of incompletely separated cells. These experiments suggest that Isc1 suppresses morphological irregularities under replication stress induced by HU and MMS.

Abnormal chitin deposition in stressed isc1Δ cells

The cell wall is responsible for maintaining cell shape; therefore, morphological abnormalities may indicate alterations in cell-wall dynamics, including chitin distribution, during morphogenesis (De Groot *et al.* 2001; Roncero 2002). Because HU- and MMS-treated *isc1*Δ cells were often misshapen and had elongated buds or attached daughter cells, we investigated whether chitin deposition was altered in these cells. We stained cells with CFW that binds specifically to chitin in the cell wall. Regardless of HU treatment, wild-type cells displayed a thin line of chitin deposition on the cell wall and significant fluorescence at the bud neck (Figure 2A). Untreated *isc1*Δ cells had a similar pattern of chitin deposition (Figure 2A). However, after HU exposure, the elongated buds and chains of cells of the *isc1*Δ strain showed a high level of fluorescence at different locations on the cell surface, including the tips of the elongated buds (Figure 2A), suggesting increased chitin deposition and abnormal cell-wall architecture. Our results suggest that Isc1 is needed for proper chitin deposition or cell-wall architecture in stressed cells.

Nuclear division and bud morphogenesis in HU-treated isc1Δ cells

Wild-type cells are known to slow DNA synthesis and delay nuclear and cell division following replication stress such as that induced by HU treatment (Slater 1973). Generally DNA replication and nuclear division coordinate transition from polar bud growth to isotropic bud growth. We wanted to analyze the status of nuclear division following HU treatment of *isc1*Δ cells. After 5 hr of HU exposure, the shape of wild-type cells remained normal but nuclei were found at the bud neck (Figure 2B). Untreated *isc1*Δ cells each had a nucleus but, after HU treatment, nuclei did not divide and remained at the bud neck (Figure 2B). Although HU treatment delayed nuclear division in both WT and *isc1*Δ cells, in the majority of *isc1*Δ cells, buds continued to elongate (polar growth) in *isc1*Δ cells. The results suggest that transition from polar bud growth to isotropic growth does not occur in *isc1*Δ cells after HU treatment.

Role of Isc1 in actin dynamics during replication stress

The actin cytoskeleton plays a major role in bud growth and many other cellular events and is a key component of the

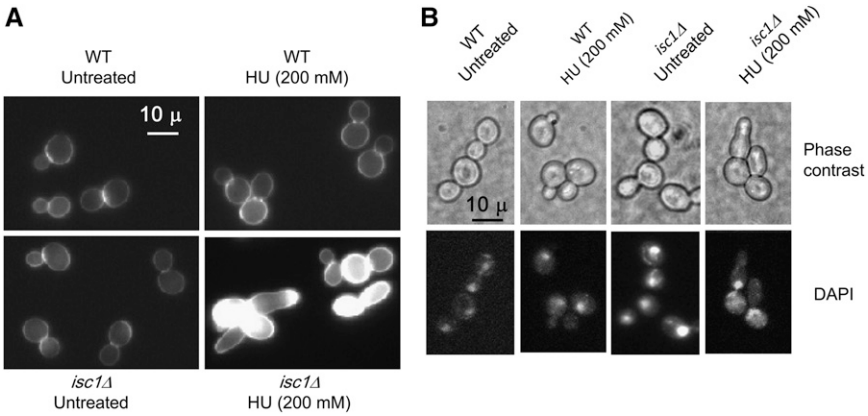

Figure 2 Cell-wall defects and DAPI staining of *isc1*Δ cells after HU exposure. (A) WT and *isc1*Δ cells treated with HU were stained with CFW (×1000-fold magnification). Only HU-treated *isc1*Δ cells display abnormal CFW staining. (B) Nucleus is stuck at the bud neck in HU-treated WT and *isc1*Δ cells while bud continues polarized growth only in the *isc1*Δ cells (phase-contrast and DAPI-stained cells, ×1000).

morphogenesis checkpoint (Lew 2003). Interestingly, actin shows a deleterious complex haploinsufficiency with Isc1 (Haarer *et al.* 2007). Therefore, we investigated whether Isc1 plays any role in actin dynamics during replication stress by HU. Rhodamine–phalloidin staining revealed that, in WT cells, the actin cytoskeleton was present as polarized cables spreading from the mother cell to the bud (Figure 3). Actin depolarization was notable after 3 hr of HU treatment (data not shown) and after 5 hr almost all cells had depolarized actin, seen as punctate staining throughout the cell (Figure 3). Rhodamine–phalloidin staining in untreated *isc1*Δ cells was identical to that of WT cells. However, HU treatment did not cause any actin depolymerization in the *isc1*Δ cells (Figure 3A). In these cells, actin cables were clearly visible and extended from mother cell to the bud tip. The results suggest that Isc1 plays an important role in actin cytoskeletal reorganization during replication stress, and it may also control cellular morphogenesis. To be sure that the lack of actin depolarization in *isc1*Δ cells was not simply due to an actin depolarization defect, but to mediation of replication stress by *isc1*Δ, we treated WT and *isc1*Δ cells with latrunculin A (LatA), a compound known to induce actin depolarization (McMillan *et al.* 1998), for 5 hr and then analyzed actin distribution. We observed punctate actin staining in both WT and *isc1*Δ cells after LatA treatment (Figure 3B), indicating depolarization. It is clear from these experiments that Isc1 controls actin depolarization in cells under replication stress.

Isc1 acts in parallel with replication checkpoint mediators to maintain cell growth and morphology

HU treatment activates the replication checkpoint (Figure 4A) and causes DNA replication arrest in an Mrc1-Tof1-Csm3-dependent manner (Katou *et al.* 2003; Bando *et al.* 2009; Tanaka *et al.* 2009) in which Csm3 forms heterotrimers with Tof1 and Mrc1 (Mayer *et al.* 2004; Xu *et al.* 2007; Bando *et al.* 2009). MMS blocks progression of the replication fork, causes DNA damage, and activates the DNA damage checkpoint through Rad9 (Putnam *et al.* 2009) (Figure 4A) as well as the S-phase checkpoint. Interestingly, Rad9 can function at the replication fork in the absence of Mrc1 or Tof1 (Foss 2001; Katou *et al.* 2003). We investigated whether the defects of HU-treated *isc1*Δ cells depend on these proteins by deleting *MRC1*, *TOF1*, *CSM3*, and *RAD9* in *isc1*Δ cells. Genome-wide studies had already shown that simultaneous deletion of *ISC1* and *CSM3* induces synthetic growth defects (Tong *et al.* 2004; Pan *et al.* 2006). We constructed *isc1*Δ*csm3*Δ, *isc1*Δ*mrc1*Δ, and *isc1*Δ*tof1*Δ strains and found them to be viable although slow growing (Supporting Information, Figure S1).

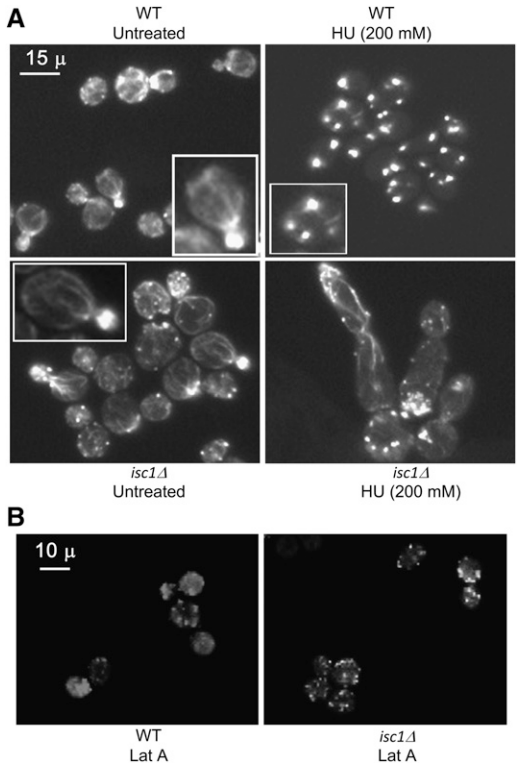

Figure 3 Defects in actin dynamics in *isc1*Δ cells with HU treatment. HU-treated cells were stained with rhodamine–phalloidin and observed at ×1000. (A) WT untreated cells have actin cables extending from mother cells to buds. After HU treatment (WT HU, 200 mM) for 5 hr, actin depolymerized (white dots). Actin cables are present in untreated *isc1*Δ cells (*isc1*Δ untreated) and in treated cells (*isc1*Δ HU, 200 mM). Insets show a magnified cell. (B) In both WT (WT LatA) and *isc1*Δ cells (*isc1*Δ LatA), actin depolymerized after 5 hr of latrunculin A treatment.

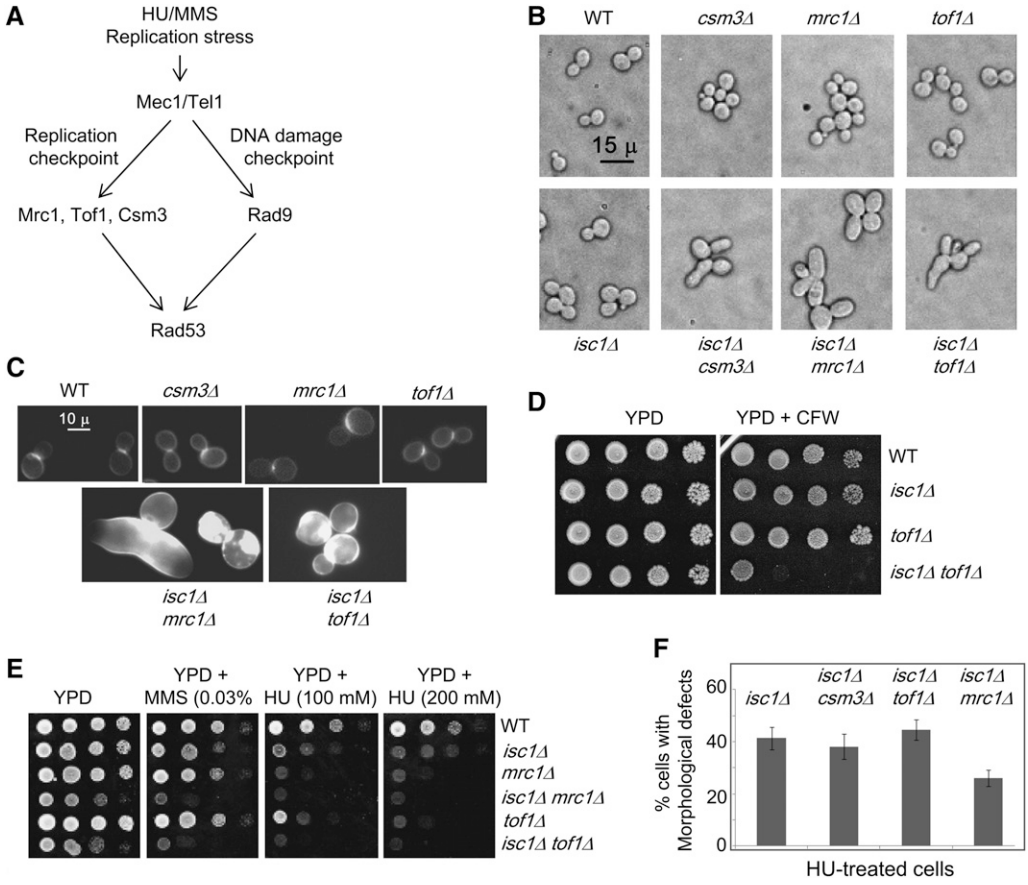

Figure 4 Genetic interactions of *ISC1* with replication checkpoint mediators *MRC1*, *TOF1*, and *CSM3* and control cell morphology. (A) Model shows the replication checkpoint and DNA damage checkpoint pathways. Mec1 and Tel1 are sensors and Rad53 is the major effector in both DNA replication checkpoint and DNA damage checkpoint (Chk1 effector is not shown). Whereas Mrc1, Tof1, and Csm3 act as the replication checkpoint mediators, Rad9 is the DNA damage checkpoint mediator. (B) Morphology of indicated strains by phase-contrast microscopy (×400). (C) CFW staining reveals cell-wall defects in *isc1*Δ*mrc1*Δ and *isc1*Δ*tof1*Δ cells. (D) Spot test with WT, *isc1*Δ, *tof1*Δ, and *isc1*Δ*tof1*Δ cells on YPD and YPD + CFW plates reveals a high sensitivity of *isc1*Δ*tof1*Δ cells to CFW. (E) Spot tests of the WT, *isc1*Δ, *mrc1*Δ, *isc1*Δ*mrc1*Δ, *tof1*Δ, and *isc1*Δ*tof1*Δ cells on YPD, YPD + 0.033% MMS, 100 mM HU, and 200 mM HU plates show that *isc1*Δ*mrc1*Δ and *isc1*Δ*tof1*Δ cells grow slowly compared with other strains and are more sensitive to HU and MMS. (F). Bars indicate the percentage of cells with HU-induced morphological aberrations (elongated buds and chains of cells) in *isc1*Δ*csm3*Δ, *isc1*Δ*mrc1*Δ, and *isc1*Δ*tof1*Δ strains compared to the *isc1*Δ strain.

Cell morphology of double-mutant strains of *isc1*Δ*mrc1*Δ, *isc1*Δ*tof1*Δ, and *isc1*Δ*csm3*Δ was assessed with and without HU treatment (Figure 4, B–F). Untreated single-mutant *isc1*Δ, *csm3*Δ, *mrc1*Δ, or *tof1*Δ strains did not display major morphological aberrations compared to untreated WT cells. However, double-mutant *isc1*Δ*mrc1*Δ, *isc1*Δ*tof1*Δ, and *isc1*Δ*csm3*Δ strains frequently formed large and sometimes misshapen mother cells and buds in comparison to WT cells and to the single-deletion derivatives even in the absence of genotoxic treatment (Figure 4B). However, some major differences were observed in cell shape and size between HU-treated *isc1*Δ cells and the untreated double-deletion strains *isc1*Δ*mrc1*Δ, *isc1*Δ*tof1*Δ, and *isc1*Δ*csm3*Δ (compare Figure 1, A and B with Figure 4B). In addition, the double-mutant strains had significant chitin accumulation in the cell wall as evidenced by enhanced CFW staining compared to staining of WT and single-mutant cells (Figure 4C). Cells with morphological aberrations are known to be sensitive to CFW (De Groot *et al.* 2001; Enserink *et al.* 2006); thus we assessed CFW sensitivity in our strains. We found that CFW sensitivity was not significantly different in WT, *isc1*Δ, or *tof1*Δ cells. However, *isc1*Δ*tof1*Δ cells were very sensitive to 25 μg/ml of CFW. We also tested *mrc1*Δ and *isc1*Δ*mrc1*Δ strains and observed that the *isc1*Δ*mrc1*Δ strain was very sensitive to low concentrations of CFW (8 μg/ml) and that the *MRC1* deletion alone caused sensitivity to higher concentrations of CFW (25 μg/ml; data not shown).

The HU sensitivity of double-mutant *isc1*Δ*mrc1*Δ, *isc1*Δ*tof1*Δ, and *isc1*Δ*csm3*Δ cells was assessed. Single-mutant *isc1*Δ, *mrc1*Δ, and *tof1*Δ cells were sensitive to both HU and MMS compared to WT cells. However, *isc1*Δ*mrc1*Δ and *isc1*Δ*tof1*Δ strains were much more sensitive to these genotoxins than was the WT strain or strains containing single deletions (Figure 4E). Notably, double-deletion strains grew slowly—even when cultures of the same absorbance were cultured on YPD plates (Figure S1). Because *isc1*Δ*mrc1*Δ, *isc1*Δ*tof1*Δ, and *isc1*Δ*csm3*Δ cells were slow growing, they were treated with a low concentration of HU (25 mM) to preserve viability while we assessed their morphology. As expected from analyses of untreated double-mutant strains, HU treatment induced severe morphological defects, including increased cell size, elongated buds, and chains of connected cells in *isc1*Δ*mrc1*Δ, *isc1*Δ*tof1*Δ, and *isc1*Δ*csm3*Δ cells (Figure 4F). However, whereas the extent of cell elongation and chain formation in the HU-induced *isc1*Δ*tof1*Δ (n = 440 cells) and *isc1*Δ*csm3*Δ (n = 278 cells) cells was not less than that of HU-treated *isc1*Δ cells, the HU-treated *isc1*Δ*mrc1*Δ cells (n = 314 cells) showed ∼30% less bud elongation and chain formation than the HU-treated *isc1*Δ cells (n = 415 cells); all the HU-treated double-mutant cells

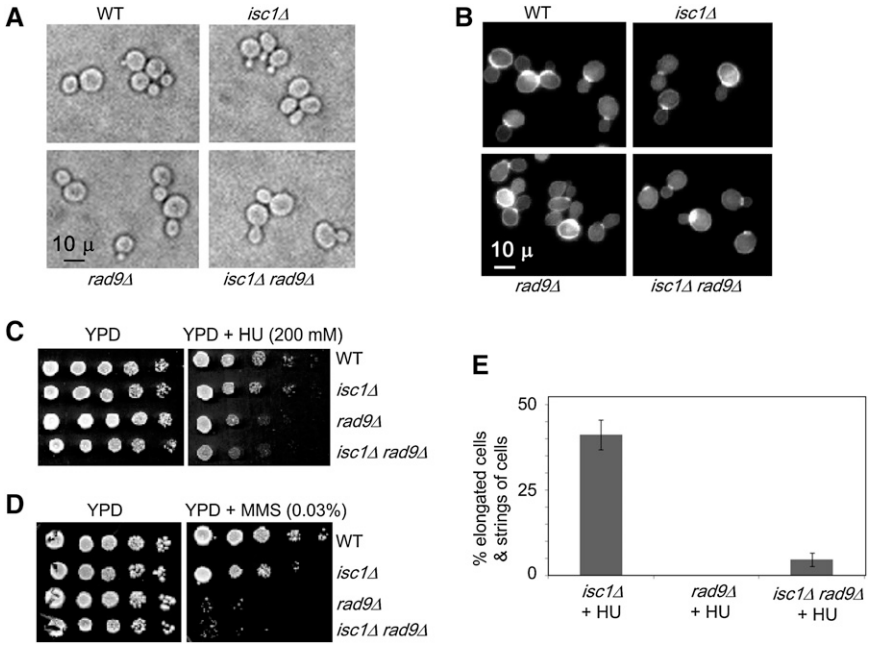

Figure 5 Signals generated in *isc1*Δ cells after HU treatment pass through Rad9 to control cellular morphology. (A) Phase-contrast microscopy (×1000) revealed no morphological aberrations of *isc1*Δ*rad9*Δ cells when compared to WT, *isc1*Δ, or *rad9*Δ cells in the absence of genotoxic treatment. (B) CFW staining of the cell wall does not differ among WT, *isc1*Δ, *rad9*Δ, and *isc1*Δ*rad9*Δ cells without genotoxic treatment. (C and D) Spot tests of serial dilutions of WT, *isc1*Δ, *rad9*Δ, and *isc1*Δ*rad9*Δ cells on YPD, YPD + HU, and YPD + MMS plates showing that *isc1*Δ*rad9*Δ cells are sensitive to both HU and MMS. (E) Bars show reduction in HU-induced morphological aberrations in *isc1*Δ*rad9*Δ cells in comparison to *isc1*Δ cells.

were bigger in size than the HU-treated *isc1*Δ cells. The results suggest that the absence of *MRC1* partially compromised HU-generated signal transduction. These results suggest that Tof1 and Csm3 do not play a role in the morphological defects of HU-treated *isc1*Δ cells, whereas Mrc1 may play a minor role in promoting bud elongation and chain formation following HU treatment. Although the morphological aberrations in double-mutant strains are somewhat different from the HU-induced defects in *isc1*Δ cells, we conclude that Isc1 acts in parallel with the replication checkpoint mediators to maintain cell growth and morphology in the absence of genotoxic treatment.

Rad9 mediates signals of replication stress in isc1Δ cells

Although Mrc1 is the main replication checkpoint mediator functioning in HU treatment, Rad9 is known to function in its absence (Katou *et al.* 2003). To explore a possible role for Rad9 in cellular signaling during replication stress, an *isc1*Δ*rad9*Δ strain was constructed and characterized. The growth pattern of the double-mutant strain was reduced compared to wild type or either single-mutant strain (Figure S2), but its cellular morphology (Figure 5A) and CFW staining pattern (Figure 5B) were normal. Both the *isc1*Δ*rad9*Δ strain and *rad9*Δ strain were sensitive to HU and MMS (Figure 5, C and D). Because these cells were highly sensitive to HU, we tested various concentrations of HU to identify a low concentration that induced morphological aberrations in *isc1*Δ cells without killing the *rad9*Δ and *isc1*Δ*rad9*Δ cells. It was observed that 25 mM HU was sufficient to induce morphological aberrations in *isc1*Δ cells. When cells were treated with 25 mM HU, WT and *rad9*Δ cells displayed no morphological irregularities (n = 214 cells; data not shown) whereas *isc1*Δ cells had severe morphological defects in 41% of the cells (n = 415 cells; Figure 5E). Interestingly, significantly fewer *isc1*Δ*rad9*Δ cells—only 4.6%—displayed morphological defects, and cells remained viable (n = 277 cells). Following treatment with 100 mM HU, we found that, whereas ~64% of *isc1*Δ cells had morphological defects, only ~12% of *isc1*Δ*rad9*Δ cells had similar defects (data not shown). These results suggest that Rad9 plays an important role in the transmission of replication stress signals generated in HU-treated *isc1*Δ cells.

Role of Rad53 in HU sensitivity and morphological aberrations of isc1Δ cells

We explored the possible involvement of the Rad53 effector in this pathway for the following reasons: (1) HU and MMS activate DNA integrity checkpoints in which signals from Mrc1-Tof1-Csm3-Rad9 converge at the effector protein Rad53 (Alcasabas *et al.* 2001; Foss 2001); (2) a reduction of cellular Rad53 concentration causes increased HU sensitivity of WT cells (Cordon-Preciado *et al.* 2006); (3) Rad53 has been shown to control cellular morphology through Swe1 activity (Enserink *et al.* 2006; Smolka *et al.* 2006; Diani *et al.* 2009); and finally, (4) *RAD9*, implicated (above) in this pathway, is an activator of *RAD53*. To investigate the role of Rad53, we transformed either an empty vector or a vector carrying *RAD53* into WT and *isc1*Δ strains. As expected, WT cells containing the vector alone were resistant to HU; however, WT cells carrying an extra copy of *RAD53* had modestly increased resistance to HU. Similarly, whereas *isc1*Δ cells with an empty vector were sensitive to HU, *isc1*Δ cells containing an extra copy of *RAD53* showed a modest increase in resistance to HU (Figure 6A). These data suggest that *RAD53* dosage partially controls HU sensitivity of *isc1*Δ cells.

We conducted a quantitative analysis of the effects of an extra copy of *RAD53* on the HU sensitivity of *isc1*Δ cells.

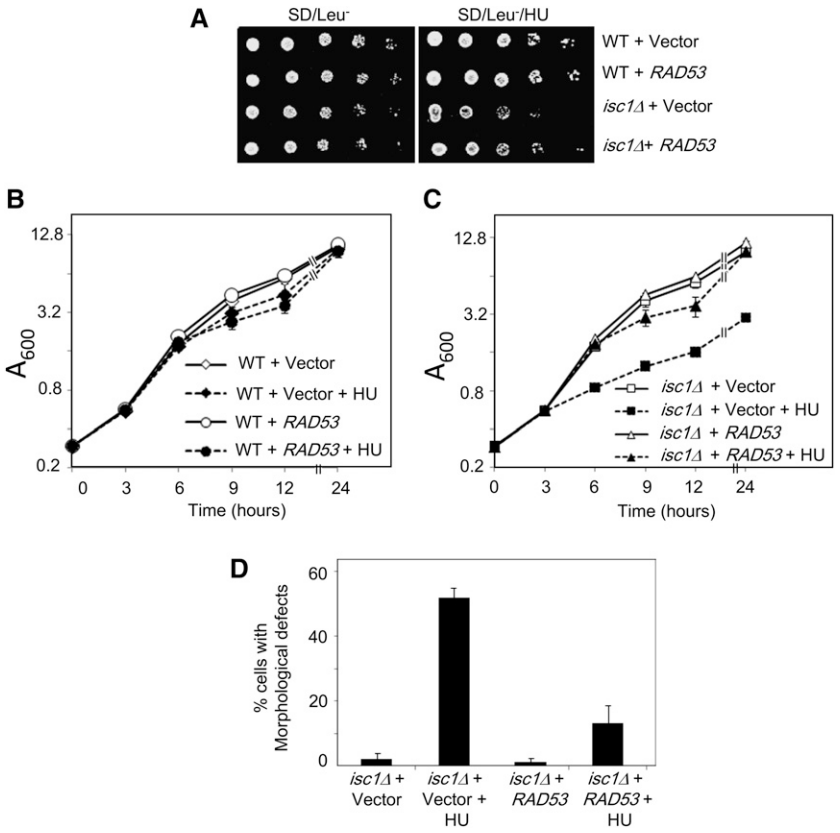

Figure 6 Increase in *RAD53* dosage rescues HU sensitivity and HU-induced morphological aberrations of *isc1*Δ cells. (A) WT and *isc1*Δ cells were transformed with empty vector pRS315 or a plasmid containing a WT *RAD53* gene expressed under the endogenous promoter. Fivefold dilutions of log-phase cells were spotted on SD/Leu$^-$ and SD/Leu$^-$/HU and incubated at 30°. Both WT and *isc1*Δ cells containing *RAD53* had increased resistance to HU compared to cells containing the empty vector. (B) WT cells containing either an empty vector or a *RAD53* plasmid were grown in SD/Leu$^-$ and SD/Leu$^-$/HU liquid media, and absorbance of all cultures was monitored at 0, 3, 6, 9, 12, and 24 hr. Vector, Control plasmid; *RAD53*, a plasmid containing an extra copy of *RAD53* gene. (C) The *isc1*Δ cells were grown and analyzed as in B. (D) *isc1*Δ cells containing either an empty vector or a *RAD53* plasmid were grown in SD/Leu$^-$ and SD/Leu$^-$/HU liquid media (*isc1*Δ cells + vector, $n = 261$; *isc1*Δ cells + vector + HU, $n = 368$; *isc1*Δ cells + *RAD53* + HU, $n = 381$; *isc1*Δ cells + *RAD53* + HU, $n = 403$). Cells were collected 22 hr after HU exposure, fixed with formaldehyde, and analyzed for morphological aberrations by phase-contrast microscopy (×400).

Because HU slows DNA replication and growth, WT cells carrying an empty vector or an extra copy of *RAD53* had a slower growth rate after HU exposure compared to untreated cells (Figure 6B). However, by 24 hr, cells exposed to HU reached the concentration of the untreated cells as the untreated cells slowly reached the stationary phase. In contrast, *isc1*Δ cells containing only the chromosomal copy of *RAD53* had severely reduced growth (75%) when exposed to HU compared to untreated cells. An extra copy of *RAD53* restored the growth of cells treated with HU to the degree of untreated cells by 24 hr (Figure 6C). We calculated the generation times of the cultures during a 3- to 6-hr growth period and observed that *isc1*Δ cells containing an empty vector had generation times of ~1.8 and 4.8 hr without HU and with HU treatment, respectively. In contrast, *isc1*Δ cells carrying a *RAD53* plasmid showed a generation time of ~1.8 hr in HU during the same time period. These experiments also indicate a role for Rad53 in the growth of *isc1*Δ cells in HU.

We also assessed the effect of *RAD53* gene dosage on cellular morphology after HU treatment. Whereas *isc1*Δ cells containing the chromosomal copy of *RAD53* displayed increased morphological aberrations (in 52% of cells), an additional copy of *RAD53* significantly reduced their HU-induced morphological irregularities to only 13% of cells (Figure 6D). We found such differences not only after 22 hr of HU exposure but also after 6 or 12 hr of HU exposure. To confirm that the extra copy of *RAD53*, and not a mutation in the *isc1*Δ cells, was responsible for these results, we grew *isc1*Δ cells containing the *RAD53* plasmid from the above experiment in rich (YPD) medium for several generations to evict the plasmid and then treated the resulting cells with HU as above. These cells displayed morphological aberrations, as did *isc1*Δ cells that had always lacked *RAD53* plasmid. Results of this experiment eliminate the possibility of a second mutation in the *RAD53*-transformed *isc1*Δ cells, causing the observed phenotypes.

Role of Swe1 and Cdk1 proteins in determining cellular morphology during stress

Because stabilization of the morphogenesis checkpoint regulator Swe1 occurs in *isc1*Δ cells upon exposure to HU/MMS (Matmati *et al.* 2009), we investigated whether Swe1 is associated with morphological aberrations in *isc1*Δ cells. As expected, stabilization of Swe1 was observed in both *isc1*Δ*tof1*Δ and *isc1*Δ*mrc1*Δ cells in comparison to WT, *isc1*Δ, and *tof1*Δ strains in the absence of genotoxic treatment (Figure 7A). We also observed that morphological aberrations seen in *isc1*Δ cells upon exposure to HU were dependent on the presence of Swe1 (Figure 7, B–D). Unlike the *isc1*Δ strain, the *isc1*Δ*swe1*Δ strain did not differ in cellular morphology, CFW staining, or actin depolymerization from *swe1*Δ and WT strains (compare Figure 7, B–D *isc1*Δ*swe1*Δ with Figure 1, A and B, Figure 2, and Figure 3). We stained HU-treated *swe1*Δ and *isc1*Δ*swe1*Δ cells with DAPI and observed that most of the cells had nuclei at the

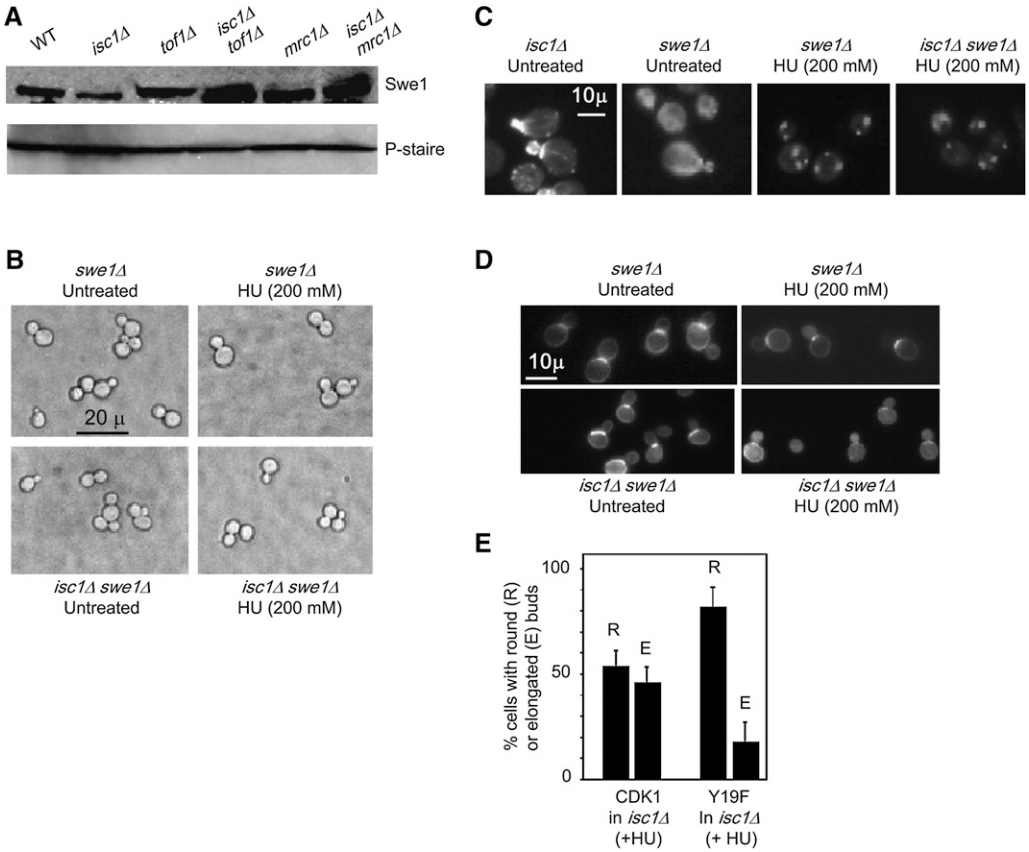

Figure 7 Role of Swe1 in determining morphology of *isc1*Δ cells under replication stress. (A) Expression profile of Swe1 in the WT, *isc1*Δ, *tof1*Δ, *isc1*Δ*tof1*Δ, *mrc1*Δ, and *isc1*Δ*mrc1*Δ strains. P-STAIRE antibody probing of the same samples shows equal loading of protein in various samples. (B) Phase-contrast microscopy reveals similar cell morphology of indicated strains regardless of HU treatment. (C) Rhodamine–phalloidin staining shows that *SWE1* deletion in *isc1*Δ cells restores actin depolymerization upon HU treatment as in WT cells. (D) CFW staining shows that *swe1*Δ and *isc1*Δ*swe1*Δ cells have no cell-wall defect. (E) Expression of the Cdk1^{Y19F} mutant, but not WT *CDK1*, rescues *isc1*Δ cells to a large extent from budding defects after HU exposure.

bud neck and no morphological irregularities (data not shown). These results suggest that the morphological aberrations in *isc1*Δ cells under replication stress require Swe1.

Because Swe1 controls G2/M arrest by inactivating Cdk1 in *isc1*Δ cells (Matmati *et al.* 2009), we tested whether the morphological aberrations of *isc1*Δ cells occurred due to inactivation of Cdk1. As expected, expression of a nonphosphorylatable mutant of *CDK1*, Cdk1^{Y19F} (Y19F, $n = 407$; in comparison to WT Cdk1, $n = 404$), in *isc1*Δ cells prevented the induction of morphological aberrations by HU to a large extent (Figure 7E). These results strongly suggest that Isc1 protein controls cellular morphology during HU exposure by destabilizing Swe1 such that Cdk1 remains active.

Isc1 functions through actin regulators during budding

Actin assembly and disassembly is regulated by proteins in more than one pathway (Pruyne and Bretscher 2000a,b; Rodal *et al.* 2005; Moseley and Goode 2006). For example, formin homologs Bni1 and Bnr1 are downstream targets of Rho proteins and function in actin cable nucleation (Imamura *et al.* 1997). Whereas Bni1 controls actin cable nucleation in the bud, Bnr1 functions at the bud neck (Pruyne *et al.* 2004). Bni1 is a member of the polarisome complex and has been implicated in bud elongation during nitrogen starvation of diploid cells (Bidlingmaier and Snyder 2004; Liu *et al.* 2010). We wanted to test whether Bni1 functions downstream of Isc1 during HU stress. *BNI1* was deleted in *isc1*Δ cells, and the resulting cells were characterized upon HU treatment. Whereas *isc1*Δ cells showed elongated buds and polarized actin, *isc1*Δ*bni1*Δ cells had shorter buds, and some cells showed a few depolarized actin spots (Figure S3A). However, the reversal was not complete, suggesting that additional proteins play a role in actin cable nucleation in *isc1*Δ cells.

To identify other proteins involved in this process, we looked to the Cdk1 pathway. Cdk1 controls actin cable organization through Cdc42 that, in turn, controls actin organization by forming a complex with Cdc42 and Bem1 (Wang 2009). *BEM1* and *ISC1* have been shown to share positive genetic interactions (Fiedler *et al.* 2009), and they may function in a common pathway to control bud morphogenesis. To test this possibility, we constructed an *isc1*Δ*bem1*Δ strain, treated it with HU, and found that bud elongation occurred much faster than in the *isc1*Δ strain (Figure S3B), suggesting that the two genes may function in parallel pathways to control bud elongation during replication stress.

To determine whether Isc1 functions through the proteins known to control actin disassembly such as cofilin, coronin, and Aip1 (Lin *et al.* 2010) during replication stress, a plasmid containing GFP-tagged *COF1* (Gandhi *et al.* 2009) was transformed into WT and *isc1*Δ cells. Following HU treatment, Cof1-GFP dynamics were compared to actin dynamics via rhodamine–phalloidin staining (Figure S3C). In untreated WT cells, actin cables spread from mother to daughter cells with the highest phalloidin staining seen in

the daughter cells; Cof1-GFP was fairly evenly distributed in mother and daughter cells. After HU treatment, actin cables in WT cells were disassembled to form punctate structures and Cof1-GFP also appeared in a punctate pattern in most cells (Figure S3C). In the *isc1*Δ cells, actin and Cof1-GFP were similarly distributed regardless of whether the cells were treated with HU (Figure S3C). All these data suggest that Isc1 functions through actin regulators to control actin depolymerization during replication stress.

Response to galactose- or butanol-induced stress is also Swe1 dependent

Because the *isc1*Δ cells displayed morphological aberrations under HU and MMS stress, we investigated whether they would show similar phenotypes under other stress conditions. Cells were grown in the presence of either galactose or butanol, both of which induced extensive morphological aberrations in *isc1*Δ cells compared to WT cells (Figure 8, A and B). It is known that a small proportion (2–3%) of WT cells display morphological aberrations after treatment with galactose (Palecek *et al.* 2002). In contrast, butanol has been shown to induce morphological aberrations in haploid WT yeast in a strain-specific manner. Although morphological aberrations were induced in Σ1278b and W303 strains, butanol did not induce aberrations in the S288c strain (Lorenz *et al.* 2000). In WT cells of the Jk9-3d ("a" type) strain used in this study, we observed morphological aberrations in <1% of cells after treatment with either galactose or butanol. However, >70% of *isc1*Δ cells displayed morphological aberrations after treatment (Figure 8, A and B).

Because we found that Swe1 controls the morphology of HU-treated *isc1*Δ cells (Figure 7), we investigated whether Swe1 plays a similar role after galactose or butanol treatment. If so, deletion of *SWE1* in *isc1*Δ cells should abolish the morphological defects. Unlike *isc1*Δ cells, neither *swe1*Δ nor *isc1*Δ*swe1*Δ cells displayed morphological aberrations after galactose or butanol treatment. These experiments show that both galactose and butanol induced morphological aberrations in *isc1*Δ cells in a Swe1-dependent manner.

These experiments, taken together, strongly suggest that, under several stress conditions, the absence of the *ISC1* gene leads to morphological defects and that these events are Swe1 dependent. Isc1 also cooperates with various DNA integrity and morphogenesis checkpoint proteins and with several actin regulators to control cellular morphology under replication stress. Finally, Rad9 and Rad53 control the HU-dependent morphological aberrations of *isc1*Δ cells.

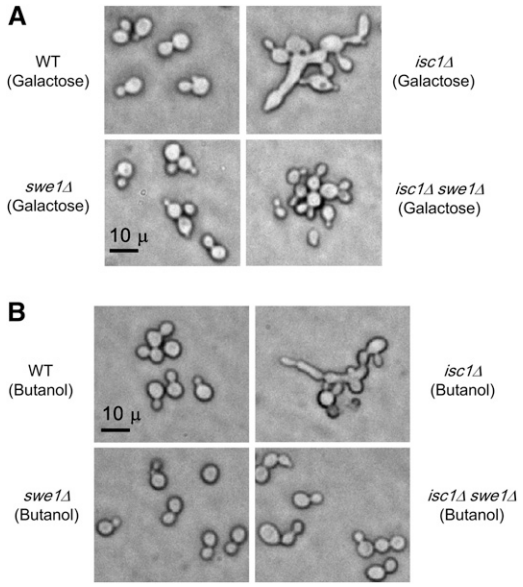

Figure 8 Galactose and butanol induce morphological aberrations in *isc1*Δ cells in a Swe1-dependent manner. (A) WT, *isc1*Δ, *swe1*Δ, and *isc1*Δ*swe1*Δ cells were grown in 2.0% D-galactose for 17 hr before fixing with formaldehyde and visualization with phase-contrast microscopy (×400). (B) WT, *isc1*Δ, *swe1*Δ, and *isc1*Δ*swe1*Δ cells were grown in 1.0% 1-butanol for 17 hr before fixing with formaldehyde and microscopic visualization (×400).

Discussion

The goal of the present study was to dissect the role of *ISC1* in determining cellular morphology during replication stress in yeast. Our results suggest that *ISC1* is a key regulator of cellular morphogenesis under a broad range of environmental stressors. The results show that the absence of *ISC1* leads to morphological aberrations, cell-wall defects, and defects in actin depolymerization during HU treatment. The replication checkpoint mediators Tof1 or Csm3 (and to a large extent Mrc1) do not play a major role in transmission of the signals generated in *isc1*Δ cells during HU treatment. However, Isc1 functions in parallel with these mediators to control cell growth and morphology in unperturbed cells. The DNA damage checkpoint mediator Rad9 was found to control signals generated by HU treatment in *isc1*Δ cells, leading to morphological defects. The checkpoint effector Rad53, activated by Rad9 upon DNA damage, also controls HU-dependent morphological aberrations of *isc1*Δ cells, suggesting that DNA damage checkpoint proteins are active under these conditions. However, there is no evidence that the DNA damage checkpoint itself controls morphology. Interestingly, Swe1 and Cdk1 were found to control morphological defects of *isc1*Δ cells. Finally, the role of *ISC1* in cellular morphology was not limited to replication stress; this sphingolipid gene was also found to control cell morphology under other stress conditions such as during galactose or butanol treatment.

We find that Rad9 and Swe1 function differently to control morphology in response to HU stress in *isc1*Δ cells. Deletion of *RAD9* reduced morphological aberrations to a large extent in *isc1*Δ cells during HU stress. In *C. albicans*, genotoxin-induced morphological aberrations are reduced by *RAD9* deletion (Shi *et al.* 2007). Rad9 is known to cause G2/M arrest upon DNA damage, and *rad9*Δ cells are MMS/HU sensitive. Although *isc1*Δ*rad9*Δ cells had fewer morphological defects at low HU concentrations, they are not resistant

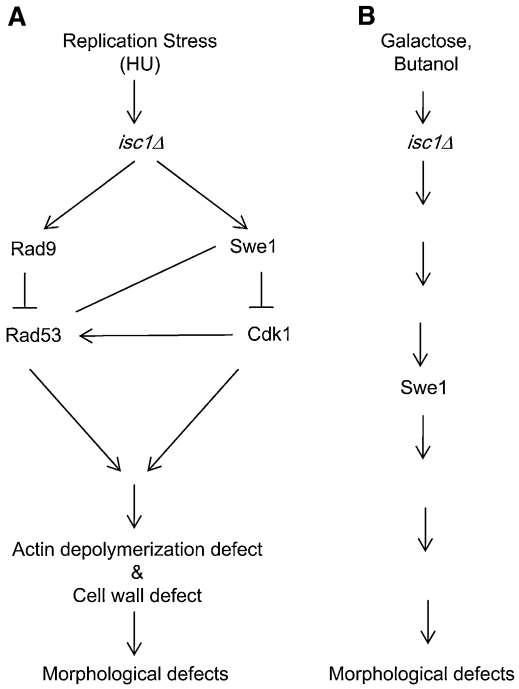

Figure 9 Model depicts mechanisms by which morphological defects are induced in *isc1*Δ cells under stress conditions. (A) In one pathway, HU treatment of *isc1*Δ cells generates signals that are recognized by Rad9 and passed to Rad53, inhibiting the latter and leading to overproduction and/or stabilization of Swe1. This leads to Cdk1 phosphorylation and inactivation, resulting in a G2/M arrest and defects in actin dynamics. Furthermore, *ISC1* gene deletion causes cell-wall defects under HU stress. The combination of the actin defect and the cell-wall defect leads to morphological aberrations. Alternatively, HU treatment of *isc1*Δ cells leads to stabilization of Swe1, which inactivates Cdk1; also HU treatment of *isc1*Δ cells causes signaling through Rad9 and Rad53. Both Cdk1 and Rad53 (see parallel pathways in Figure 9A) pathways finally lead to actin and cell-wall defects, causing morphological aberrations. Finally, Cdk1 is known to phosphorylate Rad53 to control cellular morphology. In *isc1*Δ cells, this pathway may also be active (arrow from Cdk1 to Rad53). The role of Mrc1, Tof1, and Csm3 is not shown. (B) Galactose or butanol treatment of *isc1*Δ *cells* causes Swe1 stabilization that, in turn, causes morphological aberrations.

to HU because *rad9*Δ cells are also partially sensitive to HU. In contrast, *isc1*Δ*swe1*Δ cells showed no morphological defects as well as increased HU resistance. Although both Swe1 and Rad9 control HU-induced morphological aberrations in *isc1*Δ cells, we do not know if they are acting in a single pathway or in two different pathways (see Figure 9). Because our experiments demonstrate that the effect of Swe1 in *isc1*Δ cells is greater than the individual effects of Rad9, Rad53, or Cdk1, Swe1 may operate through various effector molecules to cause cell elongation in *isc1*Δ cells during HU stress.

Rad53 has been shown to control cellular morphology (Enserink *et al.* 2006, 2009; Diani *et al.* 2009). Our study shows that increasing Rad53 gene dosage decreases the morphological aberrations of *isc1*Δ cells to a large extent. How does Isc1 control Rad53? Isc1 may partially regulate Rad53 function by altering its concentration, activity, and phosphorylation status. Although it is possible that Isc1 controls the morphological functions of Rad53 through Rad9, the DNA damage checkpoint functions of Rad9 and Rad53 may or may not be involved in this process.

At present, the proteins that transmit HU-induced signals in *isc1*Δ cells to Rad9/Rad53 are not known, but two different models can explain our results. On one hand, it is possible that Isc1 controls morphological functions of Rad53 function, which in turn, may control Swe1, and ultimately control Cdk1. On the other hand, Rad53 has phosphorylation targets of Cdk1, and a specific amino acid residue on Rad53 has been implicated in its role in certain aspects of morphogenesis (Diani *et al.* 2009). It has been shown that both Swe1 and Cdk1 control HU-mediated G2/M arrest of *isc1*Δ cell sensitivity (Matmati *et al.* 2009), and we show here that they control morphological aberrations of *isc1*Δ cells under HU stress. It is possible that Rad53 activity is affected in HU-treated *isc1*Δ cells through Cdk1 and Rad9 via two independent pathways. This may control Swe1 stabilization and activity in the *isc1*Δ cells. It is known that Swe1 accumulation leading to aberrant morphology occurs in both untreated and HU-treated *rad53*Δ cells (Enserink *et al.* 2006). Regulation of one or more proteins from among Rad53, Rad9, Cdk1, and Swe1 by phosphorylation is an attractive possibility since Isc1 generates ceramide that may, in turn, activate protein phosphatases. Detailed mutational analysis of *ISC1* and related sphingolipid genes is necessary to understand the possible role of the sphingolipid pathway in controlling Rad53 activity. Similarly, mutational analyses as well as biochemical analyses of Rad53 will show how Isc1 controls Rad53 activity. Experiments are underway to understand the mechanism of action of Isc1 on Rad53 function.

Our findings clearly indicate that both replication checkpoint and DNA damage checkpoint proteins play significant roles in cellular morphogenesis. Although Mrc1, Tof1, and Csm3 do not play a significant role in the morphological defects of *isc1*Δ cells upon HU exposure, simultaneous deletions of *ISC1* and *MRC1/TOF1/CSM3* caused slow growth and frequent basal morphogenetic aberrations in the absence of genotoxic treatment (albeit in a somewhat different manner than that of *isc1*Δ cells during HU stress). These findings suggest the following: (1) that *ISC1* functions redundantly with replication checkpoint mediator genes *MRC1*, *TOF1*, and *CSM3* to control cellular morphology and cell growth; (2) that Swe1 stability plays an important downstream role in this process; and (3) that Tof1 and Csm3 play key roles in cellular morphology, a role revealed in the absence of *ISC1*. Previous studies had implicated other checkpoint proteins such as Mec1 and Tel1, Mrc1 and Rad9, and Rad53 in cellular morphology (Jiang and Kang 2003; Enserink *et al.* 2006) in *S. cerevisiae* and Mec1, Rad9, and Rad53 in *C. albicans* (Shi *et al.* 2007).

Results from this study also specifically connect Isc1 to the regulation of actin cytoskeleton dynamics. Whereas wild-type cells undergo actin depolymerization upon exposure to HU, *isc1*Δ cells do not, suggesting that Isc1 controls

actin depolymerization specifically during replication stress. Several studies have shown that *ISC1* interacts genetically with actin. *ISC1* and *ACT1* genes share complex haploinsufficiency interactions, suggesting complementary roles for each of the two genes in the maintenance of cell growth and viability (Haarer *et al.* 2007). Diploid cells containing a single copy each of *ISC1* and *ACT1* show a severe growth defect, and similar defects in both cell growth and morphology also occur when the wild-type *ACT1* gene is replaced by *act1-105* or *act1-111* (Wertman *et al.* 1992; Cali *et al.* 1998; Haarer *et al.* 2007). Furthermore, defects in cell growth and actin depolarization in a *slm1*Δ*slm2*^{ts} mutant were abolished by deletion of the *ISC1* gene along with the calcineurin gene (Tabuchi *et al.* 2006). These results and the current findings suggest that Isc1 plays a key role in maintenance of the actin cytoskeleton and controls cellular morphology under DNA replication stress.

As shown by a previous work (Enserink *et al.* 2006), we observed that HU treatment caused actin depolarization in WT cells, indicated by punctuate staining (that was not seen in *isc1*Δ cells). It is possible that the punctate staining of actin is a reflection of actin patches. When actin patches switch from a polar to an isotropic pattern, no polar actin patterns or actin cables are seen. Many HU-treated *isc1*Δ cells are growing in a polar manner, and thus actin cables and high concentrations of patches in the early buds or tips of elongated cells are expected. Thus, the influence of HU on actin in *isc1*Δ cells could be indirect.

Several other sphingolipid pathway genes such as *LCB1*, *RVS161*, and *RVS167* have been implicated in actin dynamics (Munn *et al.* 1995; Zanolari *et al.* 2000). However, the finding that *ISC1* controls actin dynamics upon HU exposure is novel. Deletion of *BNI1* in *isc1*Δ cells partially abolishes the actin defect, suggesting that Isc1 plays a key role in actin depolarization in HU by affecting actin regulators. However, since deletion of *BNI1* confers only a partial effect, there are other genes playing redundant roles to control actin disruption mediated by *ISC1*. These data suggest that studies of other actin regulators are needed to determine how Isc1 might control actin dynamics under HU stress.

Isc1 also seems to play an important role in cell-wall synthesis. Chitin accumulates to high levels in the cell wall and bud tips during exposure to HU in *isc1*Δ cells as well as in *isc1*Δ*mrc1*Δ, *isc1*Δ*tof1*Δ, and *isc1*Δ*csm3*Δ cells. Isc1, along with the replication checkpoint mediators, may be involved in a cell-wall checkpoint (Harvey and Kellogg 2003). Recently, it was observed that the cell-wall synthesis gene *CWP1* was upregulated during the diauxic shift in *isc1*Δ cells (Kitagaki *et al.* 2009). In addition, deletion of the *ISC1* homolog *CSS1* in *Schizosaccharomyces pombe* caused severe cell-wall defects, including unusual accumulation of glucans in the periplasmic space, suggesting that Css1 plays a key role in cell-wall synthesis (Feoktistova *et al.* 2001). These observations strongly suggest that there is a link between sphingolipid metabolism and cell-wall synthesis in both yeast species. However, at present we do not have direct evidence of Isc1 controlling cell-wall synthesis. Moreover, changes in actin dynamics can affect cell-wall dynamics, and *isc1*Δ cells show defects in actin dynamics in HU. Thus the defect in cell walls of *isc1*Δ cells may be indirect.

Another major finding is that Isc1 regulates cellular morphology not only under HU/MMS stress, but also during galactose- and butanol-induced stress, and that Swe1 controls this response. Isc1 may act not only along with checkpoint proteins but also with or through various proteins of the cAMP and MAPK pathways to control cell morphology. Future experiments will elucidate the detailed mechanism of action of Isc1 in determining cell morphology under various stress conditions.

Our current understanding of the control of cellular morphology by Isc1 can be summarized in several models (see Figure 9). For example, in the absence of *ISC1* (Figure 9A), HU stress may act on Rad9 to control Rad53. Inhibition of Rad53 stabilizes Swe1 such that Cdk1 is inactivated. Loss of Cdk1 activity in turn causes defects in actin dynamics and cell-wall synthesis, resulting in morphological aberrations. Alternatively, HU exposure of *isc1*Δ cells can cause Swe1 accumulation (by a yet-unknown mechanism) leading to Cdk1 inactivation. In parallel, HU exposure of *isc1*Δ cells activates the Rad9-Rad53 pathway. Both pathways contribute to actin defects and cell-wall defects leading to morphological aberrations. These parallel pathways may influence each other or act independently. A third possibility is that treatment of *isc1*Δ cells with HU may also lead to Swe1 accumulation inducing Cdk1 phosphorylation, which can affect Rad53 phosphorylation. Cdk1-dependent Rad53 phosphorylation already has been implicated in morphogenesis in yeast (Diani *et al.* 2009). All three pathways may be used simultaneously to affect cell morphology also. Finally, a pathway supported by our findings suggests that deletion of *MRC1*, *TOF1*, or *CSM3* in an *isc1*Δ strain also leads to Swe1 stabilization and morphological aberrations.

In conclusion, we have shown for the first time that a sphingolipid pathway gene (*ISC1*) controls cellular morphogenesis under various stress conditions. We have further demonstrated that the DNA replication checkpoint mediators Mrc1, Tof1, and Csm3 function in parallel with Isc1 to monitor cell-wall and cellular morphology. Also, we find that the Isc1 protein coordinates the checkpoint mediator Rad9, the checkpoint effector Rad53, the stability of the morphogenesis checkpoint regulator Swe1, the activity of the cell cycle regulator Cdk1, and actin dynamics to control cellular morphology under HU stress. Finally, the Isc1 protein controls cell morphology under various stress conditions through the Swe1 protein.

Acknowledgments

We thank Bruce Goode, Dan Lew, Achille Pellicioli, David Pellman, and their laboratory members for supplying plasmids and strains; Maurizio Del Poeta and his lab members for providing microscopy facility; Elizabeth De

Stasio for her valuable time and help in preparation of the manuscript; and the anonymous reviewers for their valuable comments and advice for revising and improving the manuscript. This work was supported in part by the South Carolina Center of Biomedical Research Excellence (COBRE) in Lipidomics and Pathobiology [P20 RR17677 from National Center for Research Resources (NCRR)] for B.K.M. and W.J.Z., an American Cancer Society–Institutional Research Grant (ACS-IRG 97-219-08) from the Hollings Cancer Center at the Medical University of South Carolina for B.K.M., a PhRMA foundation starter grant to W.J.Z., an American Society for Biochemistry and Molecular Biology travel grant to K.T., National Institutes of Health (NIH) grant GM063265 to N.M., and NIH grants GM43825 and GM63265 to Y.A.H.

Literature Cited

Alcasabas, A. A., A. J. Osborn, J. Bachant, F. Hu, P. J. Werler *et al.*, 2001 Mrc1 transduces signals of DNA replication stress to activate Rad53. Nat. Cell Biol. 3: 958–965.

Bando, M., Y. Katou, M. Komata, H. Tanaka, T. Itoh *et al.*, 2009 Csm3, Tof1, and Mrc1 form a heterotrimeric mediator complex that associates with DNA replication forks. J. Biol. Chem. 284: 34355–34365.

Bharucha, N., J. Ma, C. J. Dobry, S. K. Lawson, Z. Yang *et al.*, 2008 Analysis of the yeast kinome reveals a network of regulated protein localization during filamentous growth. Mol. Biol. Cell 19: 2708–2717.

Bidlingmaier, S., and M. Snyder, 2004 Regulation of polarized growth initiation and termination cycles by the polarisome and Cdc42 regulators. J. Cell Biol. 164: 207–218.

Branzei, D., and M. Foiani, 2007 Interplay of replication checkpoints and repair proteins at stalled replication forks. DNA Repair (Amst.) 6: 994–1003.

Cali, B. M., T. C. Doyle, D. Botstein, and G. R. Fink, 1998 Multiple functions for actin during filamentous growth of Saccharomyces cerevisiae. Mol. Biol. Cell 9: 1873–1889.

Calzada, A., B. Hodgson, M. Kanemaki, A. Bueno, and K. Labib, 2005 Molecular anatomy and regulation of a stable replisome at a paused eukaryotic DNA replication fork. Genes Dev. 19: 1905–1919.

Chang, M., M. Bellaoui, C. Boone, and G. W. Brown, 2002 A genome-wide screen for methyl methanesulfonate-sensitive mutants reveals genes required for S phase progression in the presence of DNA damage. Proc. Natl. Acad. Sci. USA 99: 16934–16939.

Cordon-Preciado, V., S. Ufano, and A. Bueno, 2006 Limiting amounts of budding yeast Rad53 S-phase checkpoint activity results in increased resistance to DNA alkylation damage. Nucleic Acids Res. 34: 5852–5862.

de Groot, P. W., C. Ruiz, C. R. Vazquez de Aldana, E. Duenas, V. J. Cid *et al.*, 2001 A genomic approach for the identification and classification of genes involved in cell wall formation and its regulation in Saccharomyces cerevisiae. Comp. Funct. Genomics 2: 124–142.

Diani, L., C. Colombelli, B. T. Nachimuthu, R. Donnianni, P. Plevani *et al.*, 2009 Saccharomyces CDK1 phosphorylates Rad53 kinase in metaphase, influencing cellular morphogenesis. J. Biol. Chem. 284: 32627–32634.

Enserink, J. M., M. B. Smolka, H. Zhou, and R. D. Kolodner, 2006 Checkpoint proteins control morphogenetic events during DNA replication stress in Saccharomyces cerevisiae. J. Cell Biol. 175: 729–741.

Enserink, J. M., H. Hombauer, M. E. Huang, and R. D. Kolodner, 2009 Cdc28/Cdk1 positively and negatively affects genome stability in S. cerevisiae. J. Cell Biol. 185: 423–437.

Feoktistova, A., P. Magnelli, C. Abeijon, P. Perez, R. L. Lester *et al.*, 2001 Coordination between fission yeast glucan formation and growth requires a sphingolipase activity. Genetics 158: 1397–1411.

Fiedler, D., H. Braberg, M. Mehta, G. Chechik, G. Cagney *et al.*, 2009 Functional organization of the S. cerevisiae phosphorylation network. Cell 136: 952–963.

Foss, E. J., 2001 Tof1p regulates DNA damage responses during S phase in *Saccharomyces cerevisiae*. Genetics 157: 567–577.

Futerman, A. H., and H. Riezman, 2005 The ins and outs of sphingolipid synthesis. Trends Cell Biol. 15: 312–318.

Gandhi, M., V. Achard, L. Blanchoin, and B. L. Goode, 2009 Coronin switches roles in actin disassembly depending on the nucleotide state of actin. Mol. Cell 34: 364–374.

Gimeno, C. J., P. O. Ljungdahl, C. A. Styles, and G. R. Fink, 1992 Unipolar cell divisions in the yeast S. cerevisiae lead to filamentous growth: regulation by starvation and RAS. Cell 68: 1077–1090.

Gueldener, U., J. Heinisch, G. J. Koehler, D. Voss, and J. H. Hegemann, 2002 A second set of loxP marker cassettes for Cre-mediated multiple gene knockouts in budding yeast. Nucleic Acids Res. 30: e23.

Haarer, B., S. Viggiano, M. A. Hibbs, O. G. Troyanskaya, and D. C. Amberg, 2007 Modeling complex genetic interactions in a simple eukaryotic genome: actin displays a rich spectrum of complex haploinsufficiencies. Genes Dev. 21: 148–159.

Hanway, D., J. K. Chin, G. Xia, G. Oshiro, E. A. Winzeler *et al.*, 2002 Previously uncharacterized genes in the UV- and MMS-induced DNA damage response in yeast. Proc. Natl. Acad. Sci. USA 99: 10605–10610.

Harvey, S. L., and D. R. Kellogg, 2003 Conservation of mechanisms controlling entry into mitosis: budding yeast wee1 delays entry into mitosis and is required for cell size control. Curr. Biol. 13: 264–275.

Imamura, H., K. Tanaka, T. Hihara, M. Umikawa, T. Kamei *et al.*, 1997 Bni1p and Bnr1p: downstream targets of the Rho family small G-proteins which interact with profilin and regulate actin cytoskeleton in Saccharomyces cerevisiae. EMBO J. 16: 2745–2755.

Jiang, Y. W., and C. M. Kang, 2003 Induction of S. cerevisiae filamentous differentiation by slowed DNA synthesis involves Mec1, Rad53 and Swe1 checkpoint proteins. Mol. Biol. Cell 14: 5116–5124.

Katou, Y., Y. Kanoh, M. Bando, H. Noguchi, H. Tanaka *et al.*, 2003 S-phase checkpoint proteins Tof1 and Mrc1 form a stable replication-pausing complex. Nature 424: 1078–1083.

Keaton, M. A., E. S. Bardes, A. R. Marquitz, C. D. Freel, T. R. Zyla *et al.*, 2007 Differential susceptibility of yeast S and M phase CDK complexes to inhibitory tyrosine phosphorylation. Curr. Biol. 17: 1181–1189.

Kitagaki, H., L. A. Cowart, N. Matmati, D. Montefusco, J. Gandy *et al.*, 2009 ISC1-dependent metabolic adaptation reveals an indispensable role for mitochondria in induction of nuclear genes during the diauxic shift in Saccharomyces cerevisiae. J. Biol. Chem. 284: 10818–10830.

Lee, K. S., S. Asano, J. E. Park, K. Sakchaisri, and R. L. Erikson, 2005 Monitoring the cell cycle by multi-kinase-dependent regulation of Swe1/Wee1 in budding yeast. Cell Cycle 4: 1346–1349.

Lengeler, K. B., R. C. Davidson, C. D'Souza, T. Harashima, W. C. Shen *et al.*, 2000 Signal transduction cascades regulating fun-

gal development and virulence. Microbiol. Mol. Biol. Rev. 64: 746–785.
Lew, D. J., 2003 The morphogenesis checkpoint: how yeast cells watch their figures. Curr. Opin. Cell Biol. 15: 648–653.
Lew, D. J., and S. I. Reed, 1995 Cell cycle control of morphogenesis in budding yeast. Curr. Opin. Genet. Dev. 5: 17–23.
Lin, M. C., B. J. Galletta, D. Sept, and J. A. Cooper, 2010 Overlapping and distinct functions for cofilin, coronin and Aip1 in actin dynamics in vivo. J. Cell Sci. 123: 1329–1342.
Liu, B., L. Larsson, A. Caballero, X. Hao, D. Oling *et al.*, 2010 The polarisome is required for segregation and retrograde transport of protein aggregates. Cell 140: 257–267.
Liu, H., C. A. Styles, and G. R. Fink, 1993 Elements of the yeast pheromone response pathway required for filamentous growth of diploids. Science 262: 1741–1744.
Longtine, M. S., A. McKenzie III. D. J. Demarini, N. G. Shah, A. Wach *et al.*, 1998 Additional modules for versatile and economical PCR-based gene deletion and modification in Saccharomyces cerevisiae. Yeast 14: 953–961.
Lorenz, M. C., N. S. Cutler, and J. Heitman, 2000 Characterization of alcohol-induced filamentous growth in Saccharomyces cerevisiae. Mol. Biol. Cell 11: 183–199.
Matmati, N., and Y. A. Hannun, 2008 Thematic review series: sphingolipids. ISC1 (inositol phosphosphingolipid-phospholipase C), the yeast homologue of neutral sphingomyelinases. J. Lipid Res. 49: 922–928.
Matmati, N., H. Kitagaki, D. Montefusco, B. K. Mohanty, and Y. A. Hannun, 2009 Hydroxyurea sensitivity reveals a role for ISC1 in the regulation of G2/M. J. Biol. Chem. 284: 8241–8246.
Mayer, M. L., I. Pot, M. Chang, H. Xu, V. Aneliunas *et al.*, 2004 Identification of protein complexes required for efficient sister chromatid cohesion. Mol. Biol. Cell 15: 1736–1745.
McMillan, J. N., R. A. Sia, and D. J. Lew, 1998 A morphogenesis checkpoint monitors the actin cytoskeleton in yeast. J. Cell Biol. 142: 1487–1499.
McMillan, J. N., R. A. Sia, E. S. Bardes, and D. J. Lew, 1999 Phosphorylation-independent inhibition of Cdc28p by the tyrosine kinase Swe1p in the morphogenesis checkpoint. Mol. Cell. Biol. 19: 5981–5990.
Milhas, D., C. J. Clarke, and Y. A. Hannun, 2010 Sphingomyelin metabolism at the plasma membrane: implications for bioactive sphingolipids. FEBS Lett. 584: 1887–1894.
Mohanty, B. K., N. K. Bairwa, and D. Bastia, 2006 The Tof1p-Csm3p protein complex counteracts the Rrm3p helicase to control replication termination of Saccharomyces cerevisiae. Proc. Natl. Acad. Sci. USA 103: 897–902.
Moseley, J. B., and B. L. Goode, 2006 The yeast actin cytoskeleton: from cellular function to biochemical mechanism. Microbiol. Mol. Biol. Rev. 70: 605–645.
Munn, A. L., B. J. Stevenson, M. I. Geli, and H. Riezman, 1995 end5, end6, and end7: mutations that cause actin delocalization and block the internalization step of endocytosis in Saccharomyces cerevisiae. Mol. Biol. Cell 6: 1721–1742.
Palecek, S. P., A. S. Parikh, J. H. Huh, and S. J. Kron, 2002 Depression of Saccharomyces cerevisiae invasive growth on non-glucose carbon sources requires the Snf1 kinase. Mol. Microbiol. 45: 453–469.
Pan, X., and J. Heitman, 2002 Protein kinase A operates a molecular switch that governs yeast pseudohyphal differentiation. Mol. Cell. Biol. 22: 3981–3993.
Pan, X., T. Harashima, and J. Heitman, 2000 Signal transduction cascades regulating pseudohyphal differentiation of Saccharomyces cerevisiae. Curr. Opin. Microbiol. 3: 567–572.
Pan, X., P. Ye, D. S. Yuan, X. Wang, J. S. Bader *et al.*, 2006 A DNA integrity network in the yeast Saccharomyces cerevisiae. Cell 124: 1069–1081.
Parsons, A. B., R. L. Brost, H. Ding, Z. Li, C. Zhang *et al.*, 2004 Integration of chemical-genetic and genetic interaction data links bioactive compounds to cellular target pathways. Nat. Biotechnol. 22: 62–69.
Pruyne, D., and A. Bretscher, 2000a Polarization of cell growth in yeast. J. Cell Sci. 113(Pt. 4): 571–585.
Pruyne, D., and A. Bretscher, 2000b Polarization of cell growth in yeast. I. Establishment and maintenance of polarity states. J. Cell Sci. 113(Pt. 3): 365–375.
Pruyne, D., L. Gao, E. Bi, and A. Bretscher, 2004 Stable and dynamic axes of polarity use distinct formin isoforms in budding yeast. Mol. Biol. Cell 15: 4971–4989.
Putnam, C. D., E. J. Jaehnig, and R. D. Kolodner, 2009 Perspectives on the DNA damage and replication checkpoint responses in Saccharomyces cerevisiae. DNA Repair (Amst.) 8: 974–982.
Riezman, H., 2006 Organization and functions of sphingolipid biosynthesis in yeast. Biochem. Soc. Trans. 34: 367–369.
Roberts, R. L., and G. R. Fink, 1994 Elements of a single MAP kinase cascade in Saccharomyces cerevisiae mediate two developmental programs in the same cell type: mating and invasive growth. Genes Dev. 8: 2974–2985.
Rodal, A. A., O. Sokolova, D. B. Robins, K. M. Daugherty, S. Hippenmeyer *et al.*, 2005 Conformational changes in the Arp2/3 complex leading to actin nucleation. Nat. Struct. Mol. Biol. 12: 26–31.
Roncero, C., 2002 The genetic complexity of chitin synthesis in fungi. Curr. Genet. 41: 367–378.
Sawai, H., Y. Okamoto, C. Luberto, C. Mao, A. Bielawska *et al.*, 2000 Identification of ISC1 (YER019w) as inositol phosphosphingolipid phospholipase C in Saccharomyces cerevisiae. J. Biol. Chem. 275: 39793–39798.
Shi, Q. M., Y. M. Wang, X. D. Zheng, R. T. Lee, and Y. Wang, 2007 Critical role of DNA checkpoints in mediating genotoxic-stress-induced filamentous growth in Candida albicans. Mol. Biol. Cell 18: 815–826.
Sia, R. A., E. S. Bardes, and D. J. Lew, 1998 Control of Swe1p degradation by the morphogenesis checkpoint. EMBO J. 17: 6678–6688.
Slater, M. L., 1973 Effect of reversible inhibition of deoxyribonucleic acid synthesis on the yeast cell cycle. J. Bacteriol. 113: 263–270.
Smolka, M. B., S. H. Chen, P. S. Maddox, J. M. Enserink, C. P. Albuquerque *et al.*, 2006 An FHA domain-mediated protein interaction network of Rad53 reveals its role in polarized cell growth. J. Cell Biol. 175: 743–753.
Szyjka, S. J., C. J. Viggiani, and O. M. Aparicio, 2005 Mrc1 is required for normal progression of replication forks throughout chromatin in S. cerevisiae. Mol. Cell 19: 691–697.
Tabuchi, M., A. Audhya, A. B. Parsons, C. Boone, and S. D. Emr, 2006 The phosphatidylinositol 4,5-biphosphate and TORC2 binding proteins Slm1 and Slm2 function in sphingolipid regulation. Mol. Cell. Biol. 26: 5861–5875.
Tanaka, H., Y. Katou, M. Yagura, K. Saitoh, T. Itoh *et al.*, 2009 Ctf4 coordinates the progression of helicase and DNA polymerase alpha. Genes Cells 14: 807–820.
Tercero, J. A., and J. F. Diffley, 2001 Regulation of DNA replication fork progression through damaged DNA by the Mec1/Rad53 checkpoint. Nature 412: 553–557.
Tong, A. H., G. Lesage, G. D. Bader, H. Ding, H. Xu *et al.*, 2004 Global mapping of the yeast genetic interaction network. Science 303: 808–813.
Tourriere, H., G. Versini, V. Cordon-Preciado, C. Alabert, and P. Pasero, 2005 Mrc1 and Tof1 promote replication fork progression and recovery independently of Rad53. Mol. Cell 19: 699–706.

Vaena de Avalos, S., Y. Okamoto, and Y. A. Hannun, 2004 Activation and localization of inositol phosphosphingolipid phospholipase C, Isc1p, to the mitochondria during growth of Saccharomyces cerevisiae. J. Biol. Chem. 279: 11537–11545.

Wang, Y., 2009 CDKs and the yeast-hyphal decision. Curr. Opin. Microbiol. 12: 644–649.

Ward, M. P., C. J. Gimeno, G. R. Fink, and S. Garrett, 1995 SOK2 may regulate cyclic AMP-dependent protein kinase-stimulated growth and pseudohyphal development by repressing transcription. Mol. Cell. Biol. 15: 6854–6863.

Weinert, T. A., and L. H. Hartwell, 1988 The RAD9 gene controls the cell cycle response to DNA damage in Saccharomyces cerevisiae. Science 241: 317–322.

Wertman, K. F., D. G. Drubin, and D. Botstein, 1992 Systematic mutational analysis of the yeast *ACT1* gene. Genetics 132: 337–350.

Xu, H., C. Boone, and G. W. Brown, 2007 Genetic dissection of parallel sister-chromatid cohesion pathways. Genetics 176: 1417–1429.

Zanolari, B., S. Friant, K. Funato, C. Sutterlin, B. J. Stevenson *et al.*, 2000 Sphingoid base synthesis requirement for endocytosis in Saccharomyces cerevisiae. EMBO J. 19: 2824–2833.

Zegerman, P., and J. F. Diffley, 2003 Lessons in how to hold a fork. Nat. Struct. Biol. 10: 778–779.

Communicating editor: F. Winston

GENETICS

Supporting Information
http://www.genetics.org/content/suppl/2011/08/12/genetics.111.132092.DC1

Cellular Morphogenesis Under Stress Is Influenced by the Sphingolipid Pathway Gene *ISC1* and DNA Integrity Checkpoint Genes in *Saccharomyces cerevisiae*

Kaushlendra Tripathi, Nabil Matmati, W. Jim Zheng, Yusuf A. Hannun, and Bidyut K. Mohanty

DOI: 10.1534/genetics.111.132092

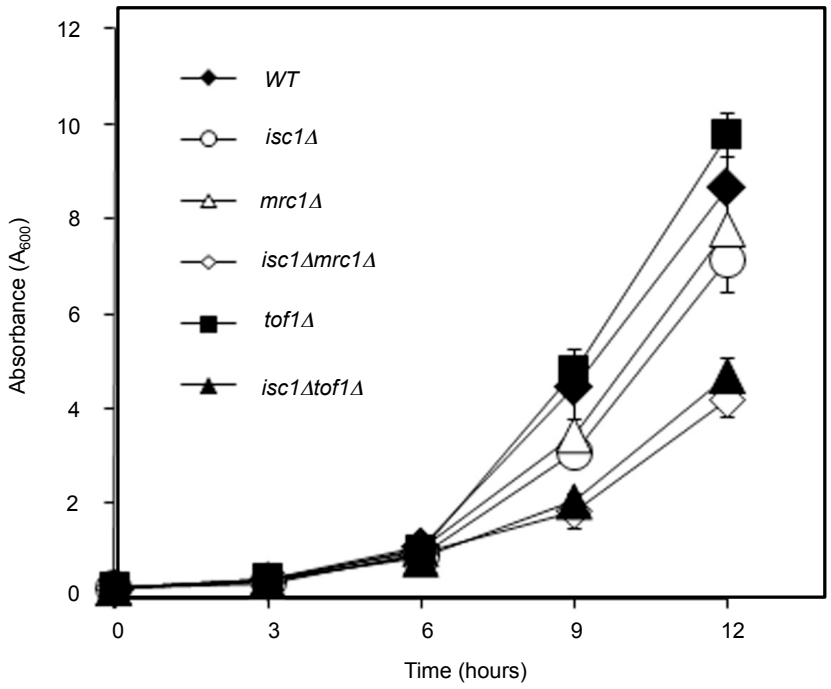

Figure S1 Growth curve of WT, *isc1Δ*, *mrc1Δ*, , *tof1Δ*,, *isc1Δmrc1Δ*, and *isc1Δtof1Δ* cells showing that *isc1Δmrc1Δ* and *isc1Δtof1Δ* cells grow slowly in comparison to other strains.

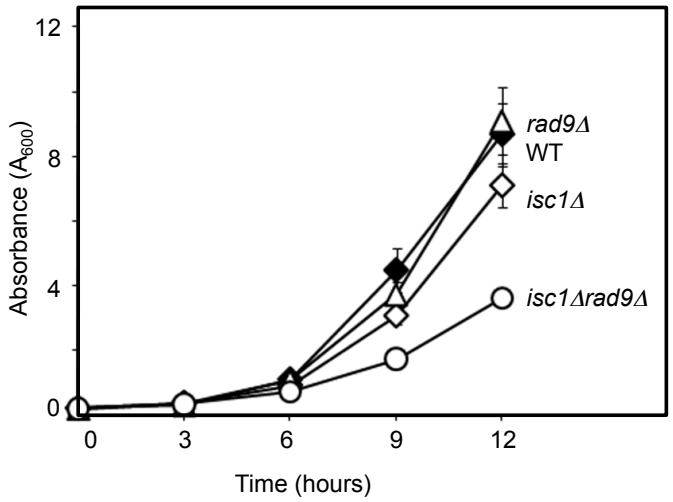

Figure S2 Growth curve of WT, *isc1Δ*, *rad9Δ*, and *isc1Δrad9Δ* cells showing that *isc1Δrad9Δ* cells are slow growing.

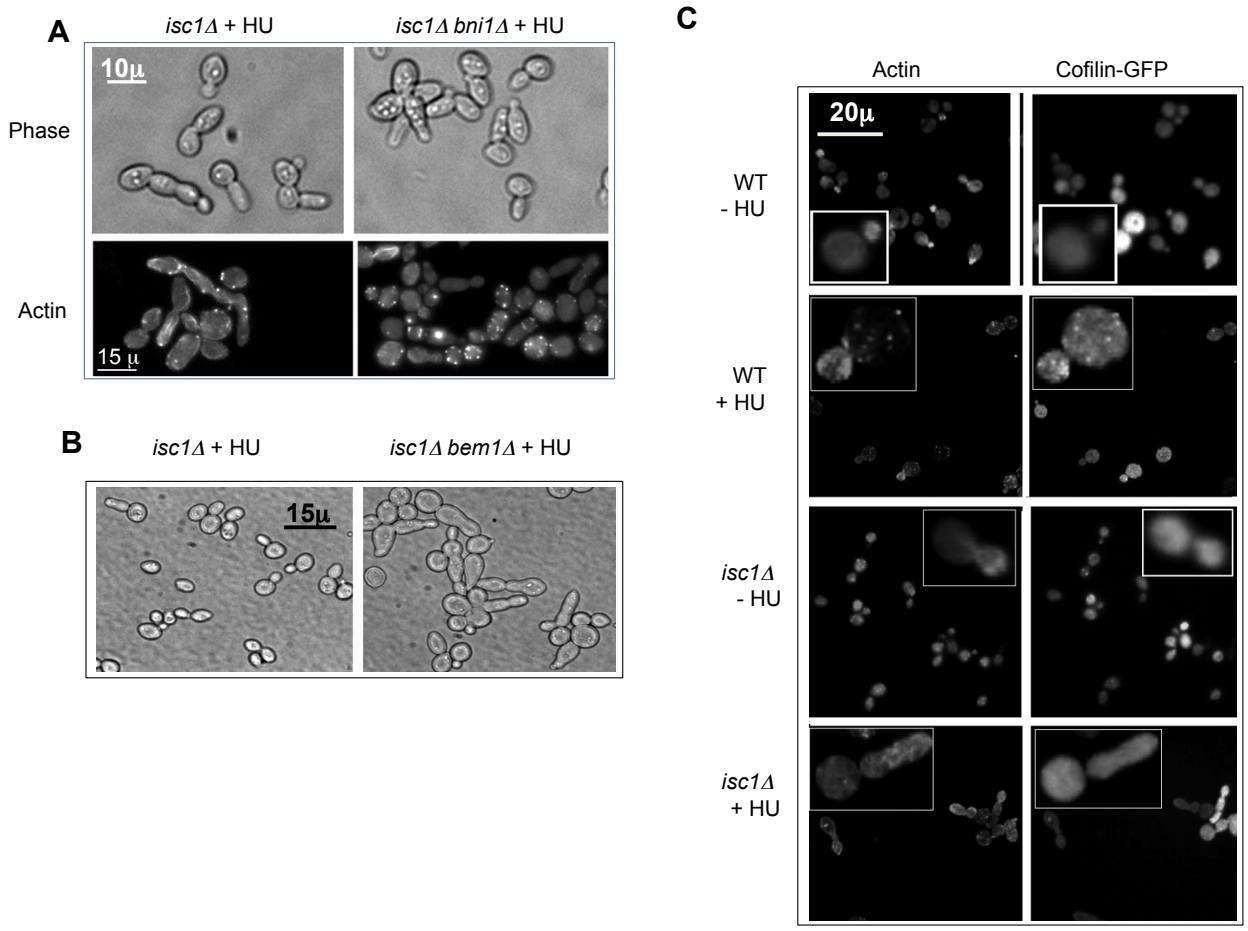

Figure S3 Analysis of possible role of *BNI1*, *BEM1*, and *COF1* in *isc1Δ* cells (A) Top: phase contrast micrographs of *isc1Δ* and *isc1Δbni1Δ* cells. (A) Bottom: Rhodamine-phalloidin staining of *isc1Δ* and *isc1Δbni1Δ* cells. (B) *isc1Δbem1Δ* cells show more severe budding defects than *isc1Δ* cells upon exposure to HU; (C) Actin (stained by Rhodamine-phalloidin) and cofilin (Cof1-GFP) showed similar patterns upon HU exposure of wild type and *isc1Δ* cells.